Design, Development, and Evaluation of a Pinch–Grasp Haptic Interface

Zoran Najdovski, *Member, IEEE*, Saeid Nahavandi, *Senior Member, IEEE*, and Toshio Fukuda, *Fellow, IEEE*

***Abstract*—Interaction with virtual or teleoperated environments requires contact with objects on a multipoint level. We describe the design of a pinch–grasp hand interface device for use as a grasping mechanism to complement haptic interfaces. To preserve a suitable level of transparency for human–computer interaction, this novel interface is designed for high-resolution contact forces, while centered around a lightweight structure. This functionality renders the device scalable and adaptable to a wide range of haptic interface structures and force level requirements. We present an optimal configuration for a pinch–grasp interface, which produces bidirectional forces to an operator's fingers and a rotational force to the wrist through a cable drive system. The device is characterized for use on a commercial haptic interface through demonstration of sustained peak performance and also workspace utilization. The dynamic performance of the pinch–grasp interface is experimentally determined, and the frequency response is identified to illustrate its contact force resolution.**

***Index Terms*—Device dynamics, grasping, haptic interface, multipoint interaction.**

I. Introduction

HAPTIC technology has advanced to perform highly stimulating and realistic interaction with virtual and teleoperated environments. Maintaining high fidelity in these devices while expanding from the current single point of contact to multiple points has proven difficult [1]. Increasing the degrees of freedom (DOFs) in highly back-drivable systems, while maintaining high fidelity and low inertia, requires extremely lightweight and high-power actuators. Development of highly dexterous grasping interfaces with high DOFs cannot be accomplished without diminishing the fundamental experience of haptic technology [2]. While a dexterous device can be outfitted with a larger sensor to actuator ratio, ultimately improving interactivity, it is by no means providing the relevant sensory stimulation for the experience.

Stimulating a human operator's sense of touch through haptic feedback should principally fulfill an intuitive exploration method. Current haptic technology imposes a reduction from a natural interaction with ten fingers to a single point of contact. This is shown to hinder haptic perception for object identification [3], [4], and ultimately reduces the sensory signals critical to manipulation tasks [5]. Identification of objects through exploration decreases in the order of free hand movement, a single outstretched finger, and five outstretched fingers [6]. The one-finger and two-finger conditions [7] demonstrated the largest difference in efficiency when varying numbers of fingers during identification tasks. The use of only one finger for the identification of common objects suffers a significant detriment in performance [7]. This suggests that the ability to extract the desired information from an object is constrained by single-point interaction, and that additional points can support the natural process to reveal particular object properties.

The problem of providing multiple points of contact for haptic grasping has been approached in different ways. A straightforward approach is multidevice utilization, by which grasping dexterity, workspace utilization, and fidelity are constrained [8]. For instance, two or more single-point haptic interfaces are used for multifinger interaction. Devices of grounded or ungrounded design are interfaced to the operator's fingers, including the forearm for ungrounded devices, to generate the required force feedback [1], [9], [10]. Although this approach can be used to realize multiple-point haptic interaction, the outcome is by no means intuitive and natural to the user due to constrained interfacing methods and potential mechanical collisions.

Force feedback hand exoskeletons have also been developed [1], [11]–[14]. For instance, Wang *et al.* explored cable drive force generation of a hand exoskeleton device. They developed a 4-DOF index finger exoskeleton that gains controlled forces from a remote actuator module. The actuator module generates bidirectional forces to each degree of freedom of the exoskeleton. Force feedback in finger extension and flexion is consequently enabled. It was stated that the ability to extend the device to the remaining fingers of the hand can be achieved; however, due to the highly complex structure, minimizing the system weight would be difficult [11]. To provide spatial force feedback, the device would require attaching to a grounded interface, therefore adding significant mass to the interface and minimizing its force capability.

Okamura *et al.* developed a pinch–grasp interface that produces grip force feedback by way of a counterweighted cable driven mechanism [2]. In this approach, the grasp interface is mounted to the distal end of a 3-DOF commercial haptic interface. Consequently, when the operator interacts with the pinch–grasp interface, they are also able to experience spatial force feedback due to the attached device. The actuator that drives the grasp mechanism is situated near the shoulder of the haptic device, and drives a single finger of the pinch–grasp

Manuscript received May 9, 2012; accepted September 5, 2012. Date of publication October 5, 2012; date of current version January 17, 2014. Recommended by Technical Editor J. Ueda.

Z. Najdovski and S. Nahavandi are with the Centre for Intelligent Systems Research, Deakin University, Geelong, Vic., 3216, Australia (e-mail: zoran.najdovski; saeid.nahavandi@deakin.edu.au).

T. Fukuda is with the Department of Micro-Nano Systems Engineering, Nagoya University, Nagoya 464-8603, Japan (e-mail: fukuda@mein.nagoya-u.ac.jp).

Digital Object Identifier 10.1109/TMECH.2012.2218662

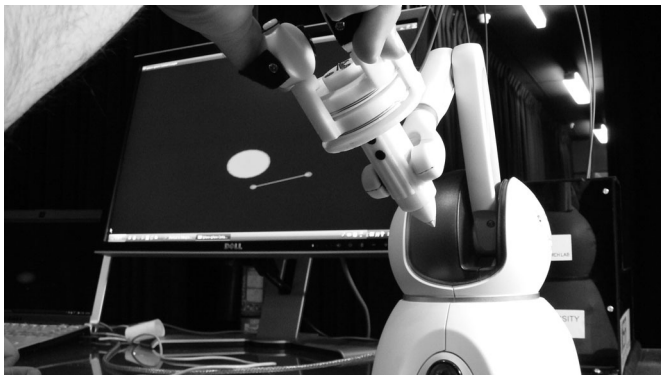

Fig. 1. Prototype haptic pinch–grasp interface attached to a Sensable Omni, interacting with a virtual sphere.

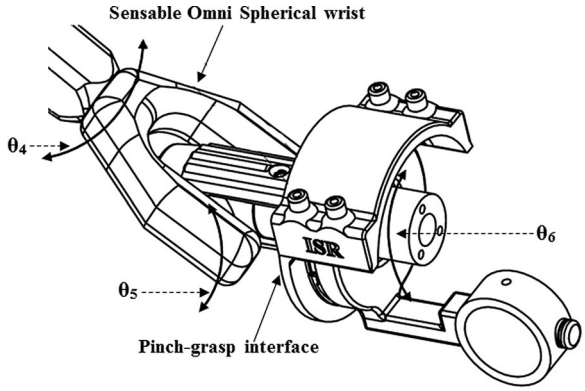

Fig. 2. Pinch–grasp interface attachment to a Sensable Omni spherical wrist.

interface. In effect, the device generates equal grasp force to the operator's grip; thus, the ability to represent independent grasp component forces, characteristic in complex dynamic objects, is constrained. This approach, however, lends itself possible to generate bidirectional forces to each finger, while reducing the effects of inertia and simultaneously adding an additional two DOFs to a commercial haptic interface.

A mechanism possessing the capabilities to increase the active DOFs, while minimizing the detrimental effects of a bulky system, would greatly benefit dextrous haptic virtual interaction. The original contribution of this study is a novel cable-driven pinch–grasp haptic interface that adds grasp capability to existing commercial haptic devices. The mechanism utilizes a cable-drive force generation system to produce bidirectional forces to an operator's fingertips [15]. The system presented here will improve on current haptic grasping interface solutions by providing a framework for high-performance force generation, for each finger to interact with virtual or teleoperated environments.

This paper describes the design, development, and analysis of the pinch–grasp haptic interface. The presented system emphasizes the need for lightweight, low-friction, and dextrous configurations for haptics technology. This paper reports on the performance of the design and highlights the tradeoffs and existing constraints in the given configuration.

II. Haptic Grasping Interface Structure

The mechanical design of the pinch–grasp interface was carried out with the objective of adding grasping capability to a commercial single-point haptic interface, while preserving transparency and delivering high-resolution contact forces. By utilizing existing low inertia, low friction, and highly back-drivable grounded haptic interfaces, the three or greater DOFs with force feedback in their design provide the foundation to build upon and extend their capabilities. As shown in Fig. 1, the pinch–grasp device provides bidirectional forces to each fingertip, as well as a rotational force to the wrist of the operator, while also providing spatial force feedback within the virtual environment. A high-dynamic (high-bandwidth) range is also required to reflect equivalent human grasp forces and consequently rigid virtual objects. Other design objectives included low inertia, low friction, high back-drivability, and zero backlash.

A. Geometry

The design of the grasping interface utilizes the kinematics and forces of a commercial haptic interface such as the Sensable Omni [16]. The Omni device is comprised of revolute joints with three DOFs incorporating force feedback, while the spherical wrist offers three DOFs with passive position feedback, shown in Fig. 2. The grasping interface comprises a revolute joint for each of the two-finger interface mechanisms, and makes use of the sixth DOF (θ_6) of the Omni device. Isolating this existing passive DOF and interfacing the grasping device to the stylus component adds two-finger points of contact with force feedback to the original commercial haptic interface. Due to the bidirectional forces of each new contact point, the sixth DOF of the Omni device becomes active, consequently providing a rotational force to the user's wrist. This outcome adds enhanced functionality within the virtual environment, specifically where manipulation of a virtual object exerts essential force components, such as rotating a screwdriver within a virtual assembly training task.

B. Grasping Interface

The proposed haptic gripper interfaces to a user through their thumb and index finger of either hand. Once in position, the users' fingers are fixed in place with straps that permit the hand to open, close, and manipulate the device within the workspace of the attached haptic interface. Two pulleys rotate on the original stylus axis of the attached haptic interface at 150° and contain arms, which are affixed to these pulleys that the operator interfaces to. To these arms, finger connection points allow the operator's fingers to naturally rotate and align with the grasp direction, as shown in Fig. 3.

The devices' actuation is generated through a cable drive system where the actuators are placed remotely, consequently eliminating actuator weight and reducing operator fatigue. As the capstan drive system is used to generate low-inertia, zero-backlash interaction forces in haptic interface designs, a cable system is used in a similar fashion to transfer forces to the user's fingertips. For each pulley on the grasping interface platform, shown in Fig. 3, a cable is routed through a low-friction nylon sheath and through the top of an outlet in the sheath attachment

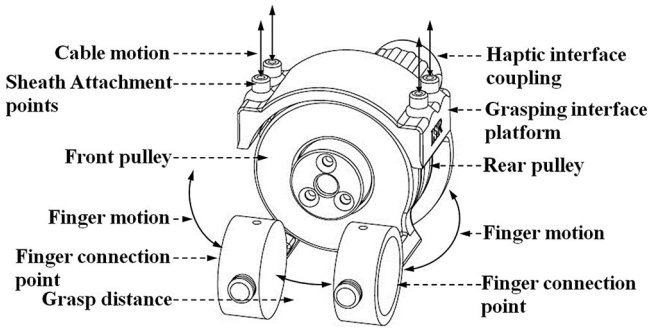

Fig. 3. Haptic pinch–grasp interface.

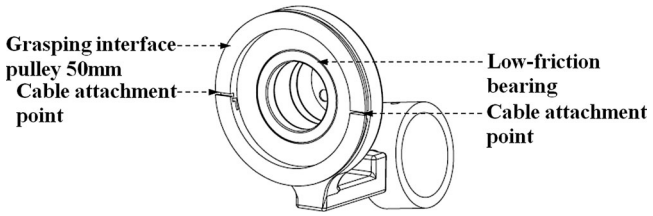

Fig. 4. Cable connection point on the pulley.

point. As shown in Fig. 4, this cable is then routed 180° around the circumference of the pulley settling in a defined channel within the pulley outer walls and attached within the cable attachment point.

The same installation procedure is performed with a second cable on the other side of the pulley and attached within the designated cable attachment point shown in Fig. 4. The placement of these cables is performed for both pulleys resulting in four separate cables. This configuration presents the basis for the bidirectional forces produced to the user's fingertips, serving to provide internal and external component forces to each finger and also a rotational force to the operator's wrist. The grasping interface platform shown in Fig. 3 is attached to a commercial haptic interface, which in this case is a Sensable Omni, and through a coupling mechanism. The design of this coupling mechanism allows the grasping interface to disengage the original passive stylus rotation (θ_6) and consequently replace it with the gripper's incorporated active DOF for both finger interfaces. Due to the remote placement of actuators, the added benefits of this design consequently produce a lightweight pinch–grasp interface that weighs 104 g.

C. Force Generation System

To produce forces to the user's fingertips while operating the pinch–grasp interface, the force generation system shown in Fig. 5 was developed. With two cables routed through individual sheaths from each pulley on the pinch–grasp interface, each cable is passed through their respective opening within the sheath attachment point and around the gripper drive mechanism, as shown in Fig. 5. This design utilizes the capstan drive assembly to provide the forces to each finger attachment point on the grasping interface through the closed-loop cable system. As the operator opens and closes the grasping interface, the cables pull

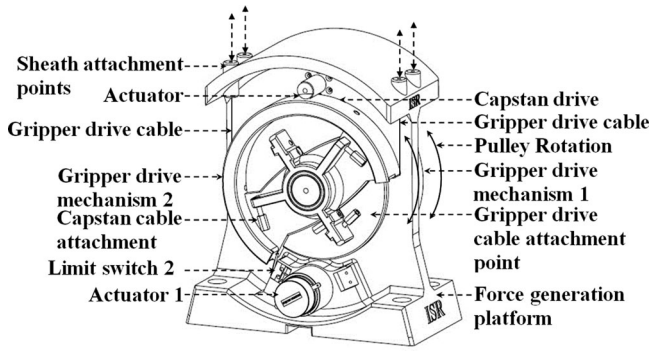

Fig. 5. Force generation system.

on each respective pulley on the force generation system and, consequently, rotate each capstan assembly.

While each actuator generates forces through their associated pulley in this assembly, these forces are transferred to the cables that are attached to a cable tensioner mechanism on their corresponding side of the drive pulley. To minimize the size of the force generation system, two actuators were placed on top and bottom of the force generation platform and facing inward as shown in Fig. 5. In this configuration, the pulleys were designed identical so that the same physical response, such as inertia, were evident to each finger on the grasping interface, and in their vertical orientation, the effects are much less apparent. As the gripper is remotely actuated, the size of the gripper and force generator's pulleys is scalable. In the current configuration, the pulley ratio is 1:2; however, either larger actuators or larger pulley ratio can produce higher performance grasp forces in the system.

Utilizing brushed DC Maxon motors, the force generation system is capable of delivering a maximum continuous force of approximately 10 N per finger, which makes it favorable to various applications that require large grasping force simulations. As the rendered force resolution by the device is dependant on the positional feedback of the mechanical system, the encoders on the force generation system have a position resolution of 0.039 mm, compared with the Sensable Omni which has a resolution of 0.055 mm [16]. The prototype grasping interface and force generation systems were developed from Acrylonitrile butadiene styrene (ABS) plastic, as it is used to make lightweight, rigid, molded products.

D. System Structure

The system structure is shown in Fig. 6. This diagram demonstrates the method used for the pinch–grasp interface to work in combination with a commercial haptic device and the force generation system, by way of the cable and sheath transmission. Modularity of this design allows for uncomplicated customization to support various haptic devices, or to enhance the output force capabilities of the force generation system through larger capacity actuators.

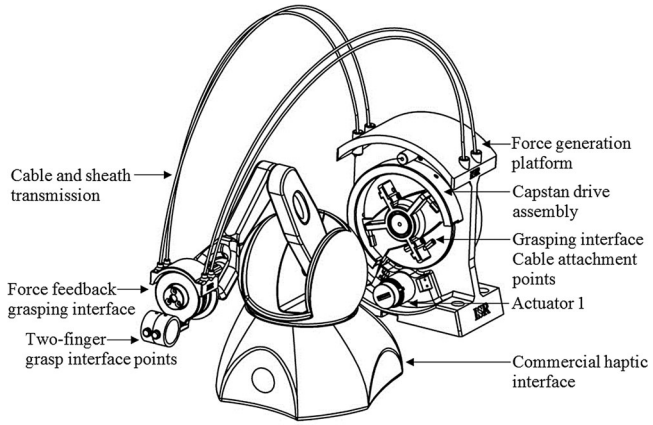

Fig. 6. System structure showing cable routing.

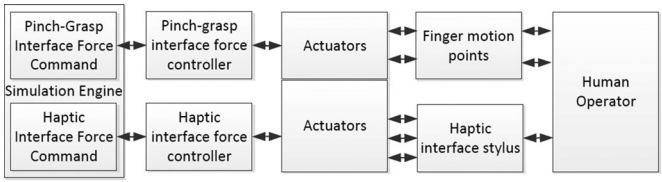

Fig. 7. System diagram demonstrating the architecture used for integration of the pinch–grasp interface onto a commercial haptic device.

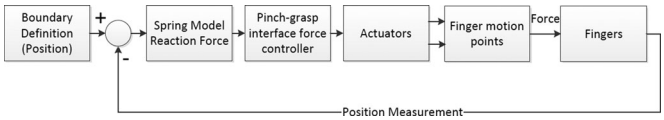

Fig. 8. Force feedback control system for the pinch–grasp interface.

E. System Architecture

The simulation engine associated with the commercial haptic device utilizes a custom library file that adds pinch–grasp capability within the virtual environment. The single point of contact from the commercial haptic device is used within the system, as shown in Fig. 7, to provide spatial force feedback such as gravitational effects and contact with other objects. This single point of contact is, therefore, virtually situated between the two points of contact from the pinch–grasp interface. The pinch–grasp device communicates via a USB interface between the force controller and the PC, and passes position and force data through this bidirectional channel, as shown in Fig. 7.

The force feedback control system of the pinch–grasp interface is shown in Fig. 8. This demonstrates the open-loop approach for rendering forces to the user's fingertips through this interface. The spring model reaction force block is composed of a wrap to zero component, which is in series with a gain (spring constant) component. The depth of penetration of the user's haptic point within the virtual object specifies the level of force feedback to the user. This depth is determined by the boundary position block in Fig. 8 and contributes to the error calculation for the final reaction force. When the difference between the boundary definition and position measurement from the interface reaches a negative value (position), a reactive spring force is generated to the user's fingertips.

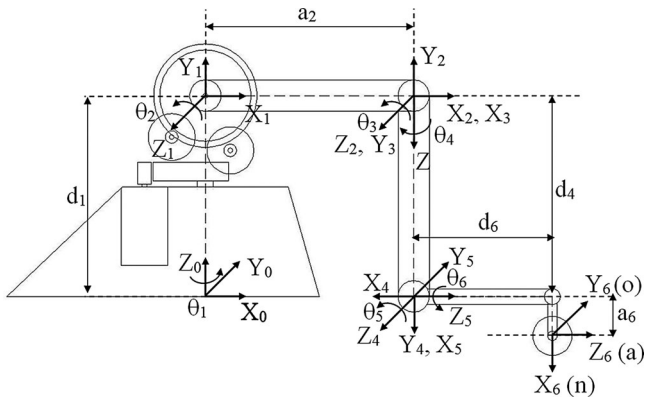

Fig. 9. Coordinate frames and mechanical structure of the Sensable Phantom Omni with the haptic pinch–grasp interface.

TABLE I
LINK PARAMETERS FOR THE HAPTIC GRASPING SYSTEM

Joint i	θ_i	α_i	$a_i(mm)$	$d_i(mm)$
1	θ_1	$\pi/2$	0	133.35
2	θ_2	0	133.35	0
3	θ_3	$\pi/2$	0	0
4	θ_4	$\pi/2$	0	133.35
5	θ_5	$-\pi/2$	0	0
6	θ_6	0	25	88.5

III. KINEMATICS

Fig. 9 illustrates the link coordinate frames and joint angles for the system used in the direct and inverse kinematic models. As each finger attachment point on the grasping interface has an associated pulley, which both share the same axis of rotation, the kinematic model is treated as a two-part model.

A. Forward Kinematics

The four parameters describing the systems' revolute joints as illustrated in Fig. 9 are represented by θ_i, d_i, a_i, and α_i.

The Sensable Omni's link and joint parameters are specified in Table I and were determined through the device's software interface and through geometric analysis.

Equations (1)–(4) make up the complete system matrix. A simplified notation is used for the direct and inverse kinematics calculations as follows: $c_1 = \cos(\theta_1)$, $c_2 = \cos(\theta_2)$, $s_1 = \sin(\theta_1)$, $s_2 = \sin(\theta_2)$, and s_{23} and c_{23} refer to $\sin(\theta_2 + \theta_3)$ and $\cos(\theta_2 + \theta_3)$, respectively. The elements p_x, p_y, and p_z represent the position of the finger interface points in the *X*-, *Y*-, and *Z*-axes, respectively, and the elements $n_{x-z}, o_{x-z}, a_{x-z}$ represent the rotation of the grasping interface. The following equations are used to independently calculate the position and orientation of the haptic pinch–grasp interface finger points as the device is geometrically uniform across the last coordinate axis:

$$n_x = c_6c_5c_4c_1c_{23} + c_6c_5s_1s_4 + c_6s_5c_1s_{23} + s_6s_4c_1c_{23} + s_6s_1c_4$$

$$n_y = c_6c_5c_4s_1c_{23} - c_6c_5c_1s_4 + c_6s_5s_1s_{23} + s_6s_4s_1c_{23} - s_6s_1c_4$$

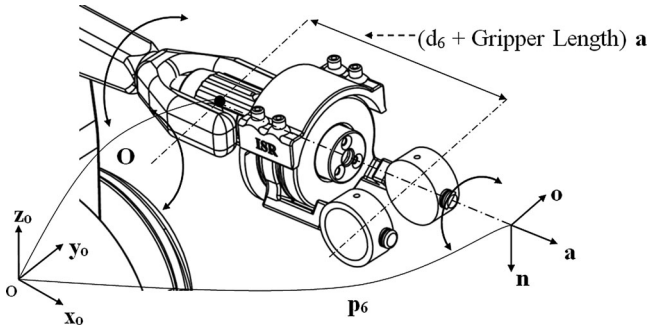

Fig. 10. Pinch–grasp interface coordinate system and [n,o,a].

$$n_z = c_6c_5c_4s_{23} - c_6s_5c_{23} + s_6s_4s_{23} \tag{1}$$

$$\begin{aligned} o_x &= s_6c_5c_4c_1c_{23} - s_6c_5s_1s_4 + s_6s_5c_1s_{23} + c_6s_4c_1c_{23} \\ &\quad + c_6s_1c_4 \\ o_y &= s_6c_5c_4s_1c_{23} - s_6c_5c_1s_4 + s_6s_5s_1s_{23} + c_6s_4s_1c_{23} \\ &\quad - c_6c_1c_4 \\ o_z &= s_6c_5c_4c_{23} + s_6s_5c_{23} + c_6s_4s_{23} \end{aligned} \tag{2}$$

$$\begin{aligned} a_x &= s_5c_4c_1c_{23} - s_5s_1s_4 + c_5c_1s_{23} \\ a_y &= s_5c_4s_1c_{23} + s_5c_1s_4 + c_5s_1s_{23} \\ a_z &= s_5c_4s_{23} - c_5c_{23} \end{aligned} \tag{3}$$

$$\begin{aligned} p_x &= a_6c_6c_5(c_4c_1c_{23} + s_1s_4) + (a_6c_6s_5c_1s_{23}) \\ &\quad - a_6s_6(s_4c_1c_{23} + s_1c_4) \\ &\quad - d_6s_5(c_4c_1c_{23} - s_1s_4) + d_6c_5c_1s_{23} + d_4c_1s_{23} + c_1a_2c_2 \\ p_y &= a_6c_6c_5(c_4s_1c_{23} - c_1s_4) + (a_6c_6s_5s_1s_{23}) \\ &\quad + a_6s_6(s_4s_1c_{23} - c_1c_4) \\ &\quad + d_6s_5(c_4s_1c_{23} + c_1s_4) + d_6c_5s_1s_{23} + d_4s_1s_{23} + s_1a_2c_2 \\ p_z &= a_6c_6c_4c_5s_{23} - a_6c_6s_5c_{23} + s_4a_6s_6s_{23} + d_6c_4s_5s_{23} \\ &\quad + d_6c_5c_{23} - d_4c_{23} + a_2s_2 + d_1. \end{aligned} \tag{4}$$

B. Inverse Kinematics

To produce the appropriate forces to the operator's fingers and hand, the inverse kinematics determines the corresponding joint angle vector $\theta = (\theta_1, \theta_2, \theta_3, \theta_4, \theta_5, \theta_6)^T$ from the known position of the fingers $p_{x_{1,2}}$, $p_{y_{1,2}}$, and $p_{z_{1,2}}$.

The joint variables for the first three joints is given by the wrist center o_c coordinates through the relation

$$o_0^c = o - d_6R \tag{5}$$

where d_6 represents the joint distance shown in Fig. 10, and R represents the orientation of the frame o_6, x_6, y_6, z_6 with respect to the base.

The values for the angles can be computed as

$$\theta_1 = \text{atan2}(p_y, p_x)$$

$$\theta_2 = \text{atan2}(f, e) \pm \text{atan2}(\sqrt{e^2 + f^2 - g^2}, g)$$

$$e = -2a_2(p_xc_1 + p_ys_1)$$

$$f = -2a_2(p_z - d_1) \tag{6}$$

$$\begin{aligned} g &= a_3^2 - a_2^2 - p_x^2c_1^2 - p_y^2s_1^2 - 2(p_xc_1) \\ &\quad p_ys_1) - p_z^2 - d_1^2 + 2p_zd_1 \end{aligned} \tag{7}$$

$$\theta_3 = \tan^{-1}\left(\frac{-s_2(p_xc_1 + p_ys_1) + c_2(p_z - d_1)}{c_2(p_xc_1 + p_ys_1) + s_2(p_z - d_1) - a_2}\right) \tag{8}$$

$$\begin{aligned} \theta_4 &= \text{atan2}(a_zs_{23} + a_xc_{23}c_1 + a_yc_{23}s_1, \\ &\quad a_zc_{23} - a_xs_{23}c_1 - a_ys_{23}s_1) \end{aligned} \tag{9}$$

$$\begin{aligned} \theta_5 &= \text{atan2}\big(o_xa_xs_1 - a_yc_1, \\ &\quad \pm\sqrt{1 - (o_xa_xs_1 - a_yc_1)}\big) \end{aligned} \tag{10}$$

$$\theta_6 = \text{atan2}(n_xs_1 - n_yc_1, o_xs_1 - o_yc_1). \tag{11}$$

IV. Dynamic Performance

Performance specifications for robotic mechanical systems typically characterize criteria such as intertia, friction, weight, and backlash in an attempt to describe these systems. Haptic interfaces rely on a bidirectional channel that can drive and be driven, which generates inconsistencies revolving around where these measurements should be taken. In robotic systems, measurements such as precision, resolution, force output, and backlash are taken from the robot's joints [17]. Hayward and Astley [18] have proposed several performance measures for characterizing the dynamic performance of a haptic interface, which include peak force, peak acceleration, inertia, and precision at the device/body interface.

A. Peak Force

The device/body interface of a haptic device is the component that allows the user to interface to, either by grasping or affixing themselves to it [18]. The peak force is measured at this interface point, and with the grasping interface is located at the finger attachment points. Hayward defines three peak force measurement categories, the long-term peak force (LTPKF), short transient peak force (STPKF), and the persistent transient peak force (PTPKF). These three cases are intended to measure the device's peak force without saturating or damaging the device. The LTPKF is carried out to understand the time taken to overheat the actuators in a worst case scenario. The haptic pinch–grasp interface was configured as shown in Fig. 11. Force measurement was achieved with a Honeywell FSG15N1A force sensor with a bandwidth of 1 kHz and a resolution of 1.0 g force. The sensor was attached to the finger interface point of the gripper and was placed directly under the intended location of an operator's index finger and thumb.

For the short transient, Hayward and Astley [18] proposed a square pulse of 10 ms as its intent is to be short enough to represent a pure impulse. The experiment for the STPKF was performed by placing the force sensor in contact with a stiff reference and applying the maximum force for a duration of 10 ms. Durations of 1 and 30 ms were also tested. These results

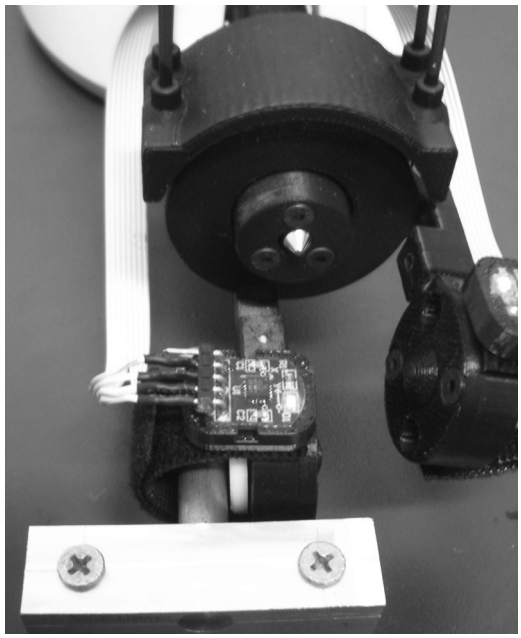

Fig. 11. Experimental setup for peak force measurement.

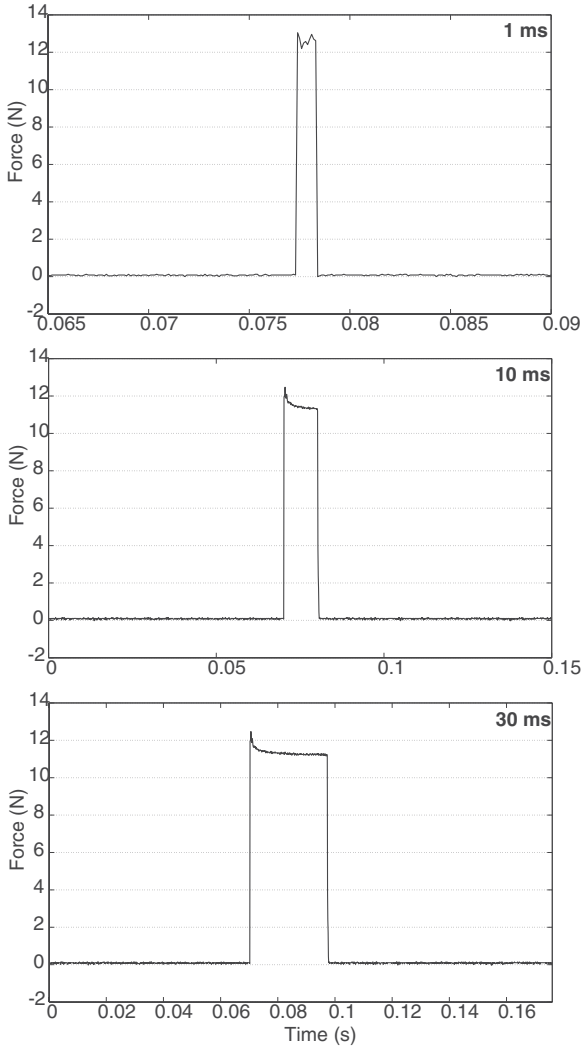

Fig. 12. Short-term peak force: 1-, 10-, and 30-ms durations.

are shown in Fig. 12, where the initial spike represents the force sensor's metallic plunger obtaining slight displacement prior to actuation of the system.

In place of the defined persistent transient force (PTPKF), the next peak force experiment relied on slowly incrementing the force level against the stiff reference. The force was increased from zero to the device's maximum force with increments of 0.07 N, and for a duration of approximately 220 ms, as shown in Fig. 13.

This experiment was designed to represent the position-based forces generated within a typical haptic virtual environment, where the results show to produce an increasingly smooth force, up to the device's maximum, and the ability to sustain this level for the duration of the experiment.

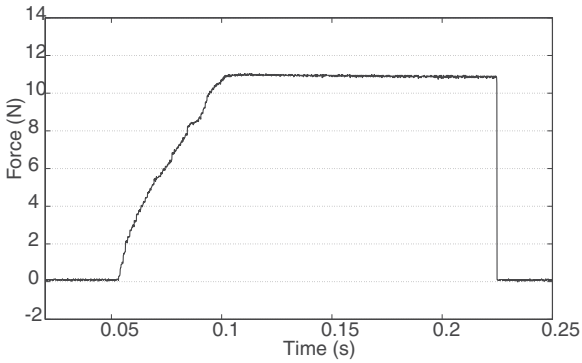

Fig. 13. 0.07-N incrementally increasing peak force.

B. Peak Acceleration

Hayward and Astley [18] have demonstrated that the acceleration capability (peak acceleration) of a haptic device is a crucial factor contributing to enhanced human–computer interaction. The haptic interface's peak acceleration was experimentally measured using an Analog Devices ADXL321 two axis accelerometer with a range of $\pm$ 18 g. The bandwidth of the built-in *RC* low-pass filter was set to 1 kHz and the voltage output of the accelerometer sampled at 10 kHz. The accelerometer was attached to the top of the finger interface points which aligns with the user's fingers, as shown in Fig. 11.

The experiment was performed on one of the two-finger interface points by actuating the pulley with a maximum force across the full range of grasp motion. As demonstrated in Fig. 14, the device reached a peak acceleration of 140 m/s^2.

C. Back-Drivability

To backdrive the pinch–grasp interface, the operator must overcome bearing friction, sheath friction, and guideway friction. Richard *et al.* [19] demonstrated a friction identification procedure involving moving the system at varying velocities of interest and recording forces from the output of their

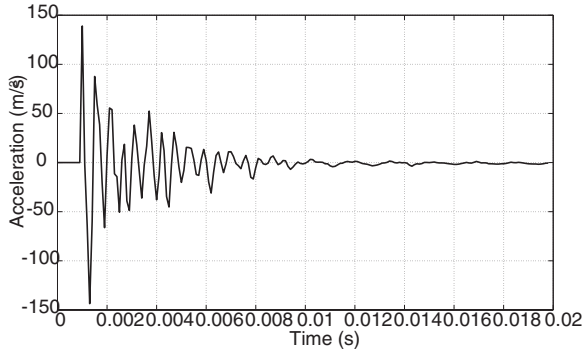

Fig. 14. Peak acceleration of the haptic pinch–grasp interface.

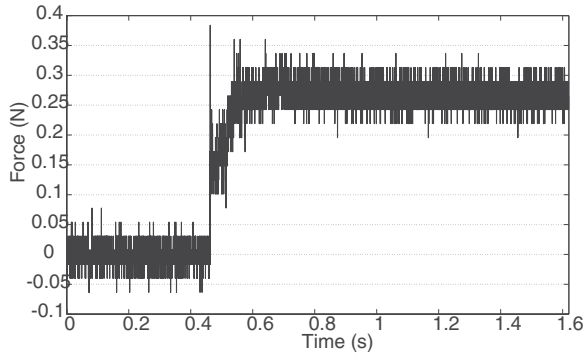

Fig. 15. Friction force of the haptic pinch–grasp interface.

linear drive configuration. Friction measurement was performed utilizing the Honeywell FSG15N1A force sensors, which was implemented on both finger attachment points. The experiment was conducted by actuating one of the finger interface arms to rotate and move the other finger interface while in contact with its force sensor. As the second interface arm is in a back-drivable state, the moving arm is actuated with an increasing force, therefore allowing the system to measure the force required to move the opposing finger interface.

Fig. 15 shows that the driving arm begins to move the opposing arm with approximately 0.27 N of force across the grasping envelope and maintains this level up until the grasping limit, which is similar to the Sensable Omni at approximately 0.26 N [16].

D. Haptic Interface Capability

Any structural addition to the end of a commercial haptic interface is likely to contribute undesirable effects upon its dynamic performance. As demonstrated in the author's previous work [15], these effects were analyzed based on a step input response of the commercial haptic interface with and without the pinch–grasp interface attached. This study extends on those results by further assessing the system response.

Attached to a Sensable Omni, the weight of the original stylus is 20 g, whereas the weight of the pinch–grasp interface is 104 g. We evaluated the system performance of the open-loop response to three-step input levels. These step inputs were based on a 20-, 30-, and 40-mm step size. These step inputs were repeated five

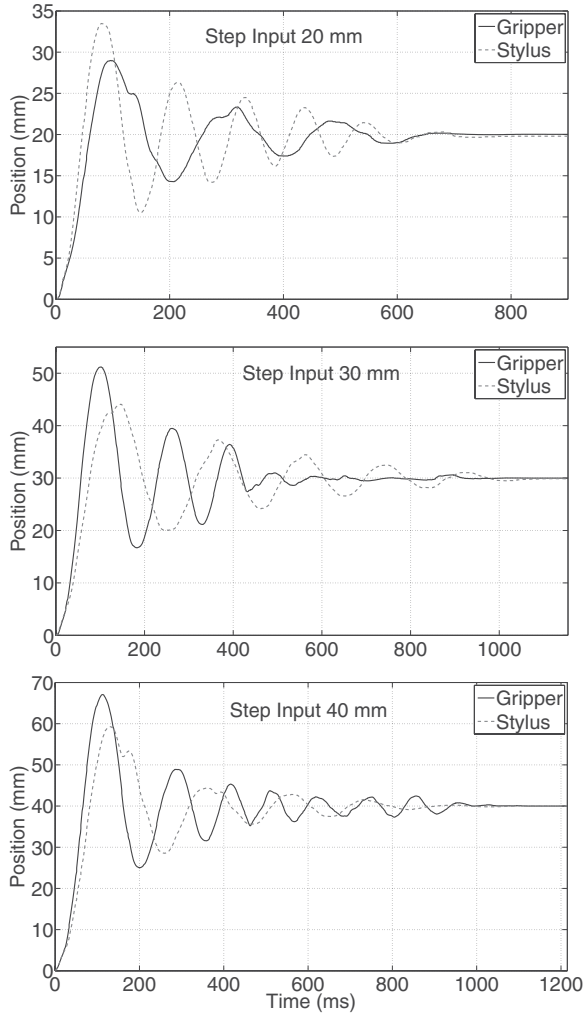

Fig. 16. Step response for the system with the pinch–grasp interface and the stylus.

times per step size and averaged. The same experiments were completed for the Sensable Omni with the original stylus, and with the pinch–grasp interface attached. In all three scenarios, it is observed that the Omni suffers from a large percentage overshoot and large settling time, as shown in Fig. 16, and consequently caused the device to fail on large positioning steps.

This failure was a result of the device exceeding its own force limits due to the extremely large percentage overshoot, and was witnessed with both the stylus and the gripper attached, as shown in Fig. 16. The settling time for the gripper is comparable to the stylus. However, with the additional weight, the gripper response does not reach as high percentage overshoot as the response with the stylus and shows a reduced oscillatory outcome.

V. Workspace Analysis

The usable workspace for a multiple device configuration (two Omni grasping configuration) compared with the workspace of the pinch–grasp system is determined to understand the workspace constraints. A single-finger attachment point was implemented on each Omni allowing an operator

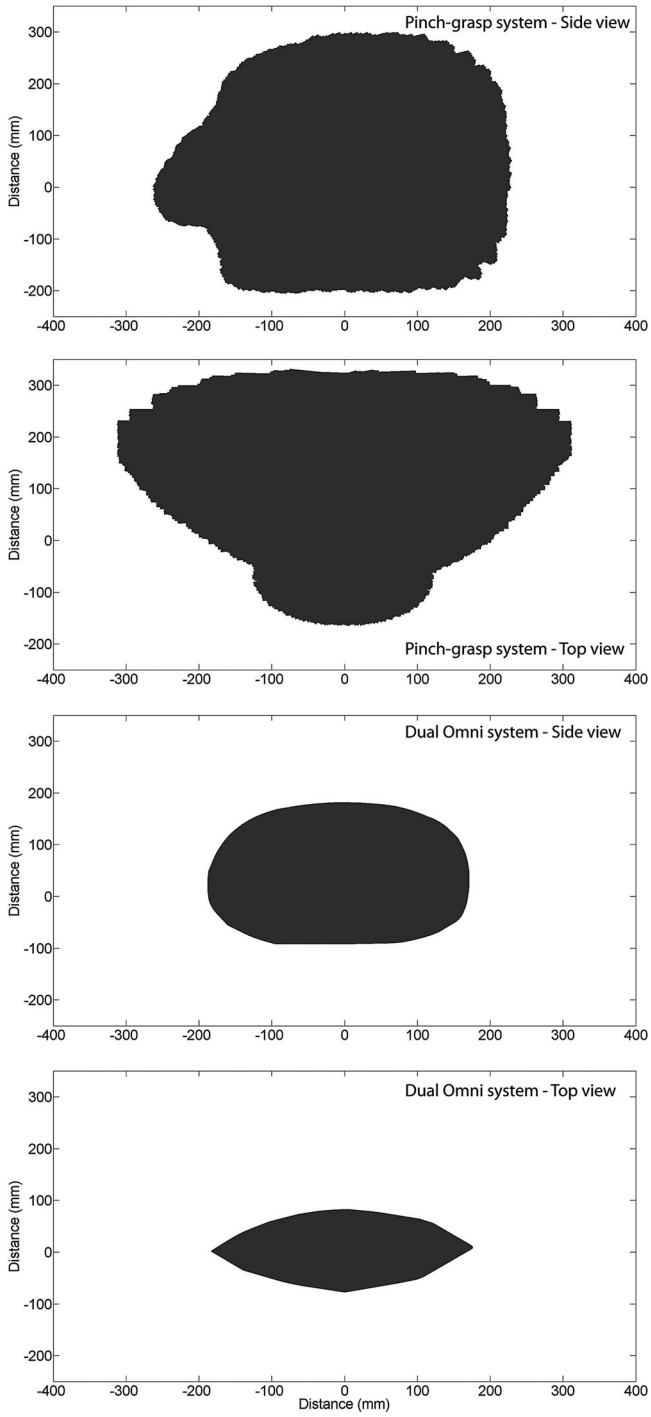

Fig. 17. Kinematic workspace of the haptic pinch–grasp interface (1 and 2) and dual Sensable Omni configuration (3 and 4) from top.

to interface their thumb and index finger, therefore replicating the pinch–grasp interface configuration. Experimental data were recorded for the dual Omni configuration, while an operator manipulated the system within the limits of the usable workspace. Fig. 17 represents the kinematic workspace of the haptic pinch–grasp interface and the usable workspace for the dual Omni configuration.

Due to Omni joint constraints, Fig. 17 shows a considerably smaller workspace in a dual Omni configuration than that of the pinch–grasp interface workspace.

VI. Structural Response

The structural response of a haptic interface is critical for identifying the fidelity of the device. Acceleration throughput [20], [21] was explored to characterize the capabilities of the pinch–grasp interface. A sinusoidal input to the gripper motor was generated by a desktop PC, where the frequency of the signal was varied in known time intervals. An accelerometer was mounted on the finger attachment point of the pinch–grasp interface, where its output was measured by a Labjack U3-HV data acquisition system.

The input signal magnitude was set to a force size of approximately 3 N, which is in the range of general pick and place force requirements. The frequency of this input signal was varied from 20 to 210 Hz with increments of 15 Hz per time interval. The experiment was run on one-finger interface point. The initial configuration of the interface was set to a position in the middle of the rotational area. The input signal was incrementally increased in frequency at approximately 0.7 s, and the experiment was completed three times for other input magnitudes slightly lower than the maximum threshold. Throughout the experiment, a user lightly placed their fingers in contact with the finger pad of the pinch–grasp interface. It was observed that the system exhibits resonance at approximately 180 Hz, which corresponds to the input force magnitude of approximately 3 N. A more detailed analysis of this approach and results is available in [22]. The normal magnitude response was analyzed for the device developed from a rigid ABS plastic material. Future work will encompass a comparison between these outcomes and the structural response of this device constructed from various other materials.

VII. Discussion

While adding only 104 g to the end of a commercial haptic device, the pinch–grasp interface is capable of providing considerable force feedback to the operator's pinch–grasp. The force and stiffness of the device may be improved even further with the use of carbon or 3-D printed metal-ceramic materials. Cable friction can be further reduced through active control input.

The pinch–grasp interface enhances the capability of current single-point haptic devices. While similar approaches have incorporated two or more haptic devices to achieve grasping capability, these suffer from potential mechanical interference and workspace constraints [8]. The presented device makes use of a single commercial system to add the same capability.

In the current configuration, the pinch–grasp interface supports two-finger interaction. Although a multifinger device design will be explored in the future, it is possible to incorporate additional DOFs to account for complete grasp closure requirements as has been implemented in similar devices [1], [11]–[14]. Alternatively, an exoskeleton design [11] presents highly complex structures and would rely on attaching the exoskeleton to a haptic interface to provide spatial force feedback. This would

ultimately result in the requirement for a commercial system with high force capabilities to support the additional mass, or the user to do so.

Other devices [2], [11] have their advantages and specific applications. However, many devices have not validated their performance, where the pinch–grasp interface design demonstrates consistent performance across the presented criteria.

VIII. Conclusion

The design, development, and evaluation of a novel pinch–grasp haptic interface have been presented. A scalable cable drive force generation system was experimentally analyzed in terms of dynamic and contact force resolution capabilities.

Through custom attachment component design, the pinch–grasp device can be interfaced to a broad range of haptic devices. A compact, scalable, and lightweight structure, adhering to transparency guidelines generates bidirectional finger and wrist forces to the operator. Workspace utilization results showed the grasping interface to be more effective compared to multihaptic interface grasping configurations.

The backdrive friction was demonstrated to be 0.27 N, which is in the region of the Sensable Omni while supporting large pinch–grasp force capabilities. Peak force and peak acceleration capabilities of the device showed respectable results at around 11 N and 140 m/s^2, respectively.

The dynamic capabilities of the Sensable Omni with the addition of the gripper were evaluated and showed only minor limitations to the device's performance.

The structural response of the system was validated by acceleration throughput experiments. The results demonstrated magnitude forces with a resonance at approximately 180 Hz.

The use of cable drive force generation for haptic interfaces has shown promising results for multipoint interaction with a scalable and highly back-drivable system.

This study aims to further investigate this design by user studies throughout virtual and teleoperation interaction. We also aim to investigate other gripper designs by enhancing the hand interface ergonomics for extended usability. We also aim to apply this interface for the manipulation of micro/nano objects including biological cells [23], [24].

References

[1] J. Blake and H. Gurocak, "Haptic glove with mr brakes for virtual reality," *IEEE/ASME Trans. Mechatronics*, vol. 14, no. 5, pp. 606–615, Oct. 2009.

[2] A. Okamura, L. Verner, T. Yamamoto, J. Gwilliam, and P. Griffiths, *Surgical Robotics: Systems Applications and Visions*. New York: Springer, 2011.

[3] G. Jansson and L. Monaci, "Haptic identification of objects with different numbers of fingers." in *Touch, Blindness and Neuroscience*, S. Ballesteros and M. A. Heller, Eds., Madrid, Spain: UNED Press, 2004, pp. 209–219.

[4] K. Kim, J. Colgate, J. Santos-Munne, A. Makhlin, and M. Peshkin, "On the design of miniature haptic devices for upper extremity prosthetics," *IEEE/ASME Trans. Mechatronics*, vol. 15, no. 1, pp. 27–39, Feb. 2010.

[5] E. B. Panarese, "Human ability to discriminate direction of three-dimensional force stimuli applied to the finger pad," *J. Neurophysiol.*, vol. 105, pp. 541–547, 2011.

[6] S. Lederman and R. Klatzky, "Haptic perception: A tutorial," *Attent., Percept., Psychophys.*, vol. 71, pp. 1439–1459, 2009.

[7] G. Jansson, "Effects of number of fingers involved in exploration on haptic identification of objects. Excerpt from pureform: The museum of pure form; haptic exploration for perception of the shape of virtual objects," Uppsala Univ., Uppsala, Sweden, Tech. Rep., 2000.

[8] G. Bttcher, D. Allerkamp, D. Glckner, and F.-E. Wolter, "Haptic two-finger contact with textiles," *Vis. Comput.*, vol. 24, pp. 911–922, 2008.

[9] A. Frisoli, F. Simoncini, M. Bergamasco, and F. Salsedo, "Kinematic design of a two contact points haptic interface for the thumb and index fingers of the hand," *ASME J. Mech. Design*, vol. 129, pp. 520–529, 2007.

[10] P. G. Robledo, J. Ortego, M. Ferre, J. Barrio, and M. Sánchez Urán, "Segmentation of bimanual virtual object manipulation tasks using multifinger haptic interfaces," *IEEE Trans. Instrum. Meas.*, vol. 60, no. 1, pp. 69–80, Jan. 2011.

[11] S. Wang, J. Li, and R. Zheng, "A resistance compensation control algorithm for a cable-driven hand exoskeleton for motor function rehabilitation," in *Intelligent Robotics and Applications*, (ser. Lecture Notes in Computer Science, vol. 6425). Berlin, Germany: Springer-Verlag, 2010, pp. 398–404.

[12] M. Lelieveld, T. Maeno, and T. Tomiyama, "Design and development of two concepts for a 4 DOF portable haptic interface with active and passive multi-point force feedback for the index finger," in *Proc. Int. Design Eng. Tech. Conf./Comput. Inf. Eng. Conf.*, Philadelphia, PA, 2006, pp. 547–556.

[13] K. Kim, Y. Nam, R. Yamane, and M. Park, "Smart mouse: 5-DOF haptic hand master using magneto-rheological fluid actuators," *J. Appl. Phys., Conf. Series*, vol. 149, no. 1, art no. 012062, 2009.

[14] M. Bouzit, G. Burdea, G. Popescu, and R. Boian, "The rutgers master ii new design force-feedback glove," *IEEE/ASME Trans. Mechatronics*, vol. 7, no. 2, pp. 256–263, Jun. 2002.

[15] Z. Najdovski and S. Nahavandi, "Extending haptic device capability for 3D virtual grasping," in *Haptics: Perception, Devices and Scenarios*, (ser. Lecture Notes in Computer Science, vol. 5024). Berlin, Germany: Springer-Verlag, 2008, pp. 494–503.

[16] *SensAble Technologies* [Online]. Available: http://www.sensable.com

[17] R. N. Jazar, *Theory of Applied Robotics Kinematics, Dynamics, and Control*, 2nd ed. New York: Springer-Verlag, 2010.

[18] V. Hayward and O. R. Astley, "Performance measures for haptic interfaces," in *Proc. 7th Int. Symp. Robot. Res.*, 1996, pp. 195–207.

[19] C. Richard, M. Cutkosky, and K. MacLean, "Friction identification for haptic display," presented at the ASME Int. Mech. Eng. Congr. Expo., Nashville, TN, 1999.

[20] V. Hayward and K. Maclean, "Do it yourself haptics: Part I," *IEEE Robot. Autom. Mag.*, vol. 14, no. 4, pp. 88–104, Dec. 2007.

[21] A. M. Okamura, M. R. Cutkosky, and J. T. Dennerlein, "Reality-based models for vibration feedback in virtual environments," *IEEE/ASME Trans. Mechatronics*, vol. 6, no. 3, pp. 245–252, Sep. 2001.

[22] Z. Najdovski and S. Nahavandi, "Characterising a novel interface for event-based haptic grasping," in *Proc. 18th IEEE Int. Symp. Robot Human Interact. Commun.*, 2009, pp. 992–997.

[23] M. Mehrtash, N. Tsuda, and M. Khamesee, "Bilateral macro-micro teleoperation using magnetic levitation," *IEEE/ASME Trans. Mechatronics*, vol. 16, no. 3, pp. 459–469, Jun. 2011.

[24] A. Fleming, "Nanopositioning system with force feedback for high-performance tracking and vibration control," *IEEE/ASME Trans. Mechatronics*, vol. 15, no. 3, pp. 433–447, Jun. 2010.

Zoran Najdovski (M'10) received the B.Eng. (Hons.) and B.Sci. degrees in mechatronics and software development in 2004, and the Ph.D. degree in 2010, all from Deakin University, Geelong, Australia.

He is currently a Postdoctoral Research Fellow at the Centre for Intelligent Systems Research, Deakin University. His research interests include the control and analysis of haptic interfaces and their contribution to human haptic perception, the development of novel haptic interface devices, and robot modeling and control.

Saeid Nahavandi (SM'07) received the B.S. (Hons), M.S., and Ph.D. degrees in automation and control from Durham University, Durham, U.K.

He holds the title of Alfred Deakin Professor, Chair of Engineering, and is the Director of the Centre for Intelligent Systems Research, Deakin University, Geelong, Australia. His research interests include robotics, haptics, and modeling of complex systems.

Dr. Nahavandi is the recipient of several national and international awards in engineering. He is an Associate Editor of the IEEE SYSTEMS JOURNAL, an IEEE Press Editorial Board Member, an Editorial Consultant Board Member of the *International Journal of Advanced Robotic Systems*, and the Editor (South Pacific region) of the *International Journal of Intelligent Automation and Soft Computing*. He was the General Co-Chair of the 2011 IEEE International Conference on Systems, Man, and Cybernetics. He is a Fellow of Engineers Australia and the Institution of Engineering and Technology, U.K.

Toshio Fukuda (F'95) received the B.S. degree from Waseda University, Tokyo, Japan, in 1971, and the M.S and Dr.Eng. degrees from The University of Tokyo, Tokyo, in 1973 and 1977, respectively.

From 1977 to 1982, he was with the National Mechanical Engineering Laboratory, Tsukuba, Japan. From 1982 to 1989, he was with the Science University of Tokyo, Tokyo. Since 1989, he has been with Nagoya University, Nagoya, Japan, where he is currently a Professor in the Department of Micro-Nano Systems Engineering. His current research interests include intelligent robotic systems, cellular robotic systems, mechatronics, and micro/nano robotics.

Dr. Fukuda was the President of the IEEE Robotics and Automation Society (from 1998 to 1999), the Editor-in-Chief of the IEEE/ASME TRANSACTIONS ON MECHATRONICS (from 2000 to 2002), the Director of IEEE Division X, Systems and Control (from 2001 to 2002), the President of the IEEE Nanotechnology Council (from 2002 to 2005), and IEEE Region 10 Director-Elect (in 2011–2012).